Int. J. Heat Mass Transfer. Vol. 16, pp. 1147–1163. Pergamon Press 1973. Printed in Great Britain

ON THE STABILITY OF NATURAL CONVECTION BOUNDARY LAYER FLOW OVER HORIZONTAL AND SLIGHTLY INCLINED SURFACES

LUCIANO PERA* and BENJAMIN GEBHART

Sibley School of Mechanical and Aerospace Engineering, Upson Hall, Cornell University, Ithaca, New York 14850, U.S.A.

(*Received* 16 *June* 1972)

Abstract—This is an analytical and experimental study of the stability of natural convection boundary layer flow adjacent to horizontal and to slightly inclined surfaces. The additional buoyancy effects resulting from small surface inclinations are taken into account. Also considered are the effect of additional buoyancy arising from the diffusion of chemical species. The limits and conditions for attached boundary flow are determined. The question of flow separation is considered.

Stability of such a flow to two-dimensional disturbances was studied by linear stability theory. Neutral stability and amplification rate contours were obtained by numerical integration of the resulting eighth-order coupled momentum and energy stability equations for air ($Pr = 0{\cdot}7$). The effect of a small surface inclination upon stability was studied using the results of a perturbation analysis of such flows. Effect of simultaneous mass diffusion on stability was also found for the case of equal Prandtl and Schmidt numbers.

Experimental verification of the stability predictions was carried out by disturbing the actual flows, over a frequency range, with a thin vibrating ribbon and observing the behavior of the convected disturbance. A Mach–Zehnder interferometer was used to study flow characteristics under both disturbed and and undisturbed conditions. The more complicated three-dimensional disturbances, which also arose, were made visible by smoke injection into the boundary region.

The stability theory predicts the correct trend of the stability limits for both horizontal and slightly inclined surfaces. However, the calculations are not in as good an agreement with observations as in flows adjacent to vertical surfaces or in freely thermal plumes. The discrepancies found are believed to result from the rapid growth of three-dimensional effects in the attached boundary-layer region and from a downstream separation-like phenomenon.

INTRODUCTION

THIS study concerns the instability, transition and separation of the natural convection flows induced by buoyancy forces over horizontal and nearly horizontal surfaces. Such flows have very interesting characteristics and occur in many circumstances, for example, in flows of micro-meterological scale. Solar heating at the surface of the earth induces a pressure gradient which results in attached flows parallel to the surface. They become unstable and may detach from the surface. Pera and Gebhart [1] report analysis and experiments for such flows. Such mechanisms inevitably arise adjacent to any heated bounding surface body of fluid. These flows locally separate and their relation to resulting cellular and updraft patterns in the ambient medium above is not at all clear at this time. However, it is suspected that, immediately above a heated bounding surface which is uneven or ridged, the general flow characteristics may be determined by the collective nature of these separating flows and not primarily by a thermal instability mechanism arising over a heated surface idealized as completely horizontal. The study reported here is an attempt to understand more about the stability of attached flow and about any separation mechanisms. Increased understanding has important implications concerning the nature of the circulations formed above surfaces.

The nature of the laminar instability in

* At present at FIAT, Direzione Ricerca, Torino, Italy.

natural convection flow adjacent to vertical surfaces and in plumes is well understood. Eventual transition to turbulence results after amplification of convected disturbances. The two-dimensional linear theory correctly predicts instability characteristics and disturbance amplification for flows near a vertical surface and even implies conditions for transition to turbulence. Gebhart [2] and Heiber and Gebhart [3] have recently reviewed what is known about such effects. Knowledge concerning such mechanisms for natural convection flow adjacent to horizontal and inclined surfaces is limited to a few experimental results and these observations lead to contradictory conclusions.

Rich [4] presented the first extensive study, both theoretical and experimental, of the heat transfer occurring in natural convection flows adjacent to inclined heated surfaces in air. A Mach–Zehnder interferometer was used to observe the two-dimensional temperature field. For surfaces inclined more than 40 degrees from the vertical position it was concluded that three-dimensional effects are important.

The first visual observations and temperature measurements over heated horizontal surfaces were made by Croft [5]. Schlieren observations indicated a cellular mode of convection near the surface which was thought to be similar to Benard cells. Above the cellular region the motion was seen to continue in rising plumes. These originated through a mushrooming effect from the upward flow of the cellular motion below.

Tritton [6] studied transition to turbulence in air in flows adjacent to a heated vertical surface and to surfaces inclined up to 50 degrees from the vertical. The range of Grashof number over which transition occurred was measured for the regions both above and below the heated plate. Inclination was found to have a stabilizing effect on the flow below the plate and a destabilizing one for the flow above. The cause and nature of the flow instability was not studied. In an earlier paper Tritton [7] studied the turbulent regime over such surfaces.

Lock, Gort and Pond [8] reported an experimental study in air of the stability of the flow adjacent to inclined heated surfaces. Flow disturbances were observed with a Schlieren system and found to be wave-like, similar to many other observations in flows adjacent to vertical surfaces. The wavelength and frequency of the disturbances were measured at given surface inclinations using thermocouple probes. The effect of the surface inclination on these quantities was small. Three dimensional properties of the flow were not determined.

Husar and Sparrow [9] studied flow adjacent to horizontal heated surfaces in water for several surface geometries. The electro-chemical visualization technique of Baker [10] was used. However, this method is subject to some uncertainty since a buoyancy effect is inevitably generated in the small gas bubbles which are produced on the surface of the plate in producing the pH shift which allows visualization. In our laboratory, we have found that the additional bouyancy effect may be large in the weak flows characteristic of natural convection. It may modify the flow or generate natural convection patterns inexistent in simple thermally induced flows. This visualization technique was applied to nearly horizontal and to slightly inclined surfaces in our lab. The bubbles of gas formed at the heated surface penetrated the attached boundary-layer and rose vertically, thus generating additional fluid circulations.

Sparrow and Husar [11] also used the electro-chemical visualization technique for a study of the mechanism of instability of flows adjacent to inclined surfaces in water. Longitudinal vortices or rolls were observed, distributed across the width of the plate. It was concluded that, contrary to the established wave mechanism of early instability in vertical flows, the longitudinal vortices are the first stage of the laminar-turbulent transition process for in-inclined surfaces.

Lloyd and Sparrow [12], again using the same method in water, studied the relationship between the inclination of the heated surface

and the apparent mechanism of flow instability. They concluded that, up to a surface inclination of 14 degrees from the vertical, the flow instability is characterized principally by two-dimensional disturbances. Following a transition zone of approximately 3 degrees, the instability mechanism was characterized by longitudinal vortices. The two modes of instability were concluded to coexist in the intermediate region. The effect that the presence of the additional buoyancy mechanism associated with the gas bubbles may have on the observed mechanisms was not considered.

The first theoretical treatment of the instability of natural convection flow over an inclined surface was carried out by Plapp [13]. The momentum and energy stability equations, were presented, including the coupling caused by the two components of the buoyancy force.

Rotem and Claassen [14] in studying the flow adjacent to horizontal heated surfaces in air with a semi-focusing Schlieren system concluded that two kinds of instability may affect such flows. The first arose from the formation of a thick boundary layer due to an insufficient driving pressure gradient, with a subsequent separation of the flow. The second might be of a kind of gravitational instability arising from a combined action of the buoyancy force and pressure gradient effects. The experiments indicated that, for horizontal surfaces, the second mechanism is the dominant one. For flow over heated horizontal surfaces they found that the third root of the local Grashof number, $Gr_x^{\frac{1}{3}}$, is as low as 100–125 for fully established eddying convection in air. The exact value was thought to depend on the size of the plate and on the temperature level. Tritton [7] had found that this value is much higher and may even reach 1100–1300 for plates inclined up to 40 degrees from the horizontal.

Hassan and Mohamed [11] experimentally determined local heat transfer parameters along isothermal flat surfaces in air for a wide range of surface temperatures and inclinations, using Boelter–Schmidt heat-flux meters. For horizontal and slightly inclined surfaces it was found that the boundary-layer apparently separates from the heated surface. Separation was inferred from the heat flux variation along the surface, under the assumption that the heat flux decreases at the location where the flow separates and is followed by quite uniform flux in the separated region.

The present work considers various aspects of the instability mechanisms of the natural convection boundary layer flow adjacent to horizontal and to slightly inclined heated surfaces in air. It is intended to bring further insight to the problem of instability and separation of such flows. Stability predictions were obtained numerically for air ($Pr = 0{\cdot}7$) for the two-dimensional flow generated by thermally induced buoyancy forces. The stability of the flow induced by the combined buoyancy effects due to thermal and chemical species diffusion was also studied. Following Gebhart and Pera [16], similarity function is defined which simultaneously accounts for both the thermal and mass diffusion buoyancy effects. It is of the same form as that found for single buoyancy mechanism flows. For equal Prandtl and Schmidt numbers it is shown that the stability characteristics calculated for purely thermal convection apply for combined buoyancy effects, when the coordinates and parameters are properly reinterpreted. Numerical results for thermally induced laminar boundary-layer flow were given by Pera and Gebhart [1], for a range of Prandtl number, for both uniform flux and temperature surface conditions. The effect of a small inclination of the surface was included by a perturbation analysis of the flow over a perfectly horizontal surface.

The experiments reported here concern disturbance behavior and separation over heated, horizontal and nearly horizontal isothermal surfaces in air at atmospheric conditions. Two surface geometries were used for the experiment. The first consisted of a simple isothermal plate with one leading edge and a removable adiabatic surface at the trailing edge.

The intent was to investigate the effect of the finite extent of the surface and of adiabatic extension at its trailing edge. The second plate, hinged at its center, permitted a symmetric geometry under all surface inclinations. The upward faced wedge-shaped surface has two leading edges and a common trailing edge. It permitted determination of both the effects of a finite length and of a second leading edge on the flow, on the occurrence of separation, on the nature of plume formation, on three-dimensional secondary flow effects and on the heat transfer in the attached laminar boundary layer. In this second configuration similar boundary layers are formed over the two surfaces and move toward the center. These layers must eventually turn away from the surface and rise either in a plume or in a cellular motion.

The two-dimensional temperature field was determined with a Mach–Zehnder interferometer. Disturbances were introduced into the boundary region with an externally controlled variable frequency vibrating ribbon. The behavior of these disturbances was observed as they were convected by the flow and their effect on the occurrence of downstream flow separation was studied. Information related to boundary-layer separation and plume formation, and its three-dimensional characteristics were also obtained by smoke visualization. These experimental observations, and the analysis of stability, have led to a better understanding of the nature of the mechanisms that cause instability and eventual separation of the flow.

THE STABILITY ANALYSIS

The flow over a heated semi-infinite flat surface inclined at a small angle θ from the horizontal and facing upward (Fig. 5) are described by the equations resulting from conservation of mass, force-momentum and energy. The equations are written in terms of velocity (u, v), temperature t, gravitational force g and dynamic or motion pressure p, in terms of the coordinates x along the surface and y normal thereto. Both x and y are opposed to the direction of the two corresponding components of the gravity force. The equations in the Boussinesq and boundary layer approximations are

$$\frac{\partial u}{\partial x} + \frac{\partial v}{\partial y} = 0, \tag{1}$$

$$\frac{\partial u}{\partial \tau} + u\frac{\partial u}{\partial x} + v\frac{\partial u}{\partial y} = -\frac{1}{\rho}\frac{\partial p}{\partial x} + \nu\left\{\frac{\partial^2 u}{\partial y^2}\right\} + g\beta(t - t_\infty)\sin\theta, \tag{2}$$

$$\frac{\partial v}{\partial \tau} + u\frac{\partial v}{\partial x} + v\frac{\partial v}{\partial y} = -\frac{1}{\rho}\frac{\partial p}{\partial y} + \nu\left\{\frac{\partial^2 v}{\partial y^2}\right\} + g\beta(t - t_\infty)\cos\theta, \tag{3}$$

$$\frac{\partial t}{\partial \tau} + u\frac{\partial t}{\partial x} + v\frac{\partial t}{\partial y} = \frac{k}{\rho c_p}\left(\frac{\partial^2 t}{\partial y^2}\right). \tag{4}$$

Following usual procedures of stability theory, an arbitrary small disturbance is superimposed on the steady primary flow such that the resulting fluid motion may be described in terms of the stream function Ψ and the temperature difference $(t - t_\infty)$, between the fluid and the distant medium, locally at x as

$$\Psi = 5\nu\left\{\frac{Gr_x}{5}\right\}^{\frac{1}{4}}\{f(\eta, x) + \phi(\eta, x)\,e^{i(\bar{\alpha}x - \bar{\beta}\tau)}\}, \tag{5}$$

and

$$t - t_\infty = \Delta T\{\Phi(\eta, x) + s(\eta, x)\,e^{i(\bar{\alpha}x - \bar{\beta}\tau)}\}, \tag{6}$$

where the first term in each equation is the steady laminar flow. The quantity $\bar{\beta} = 2\pi f$ is taken to be real, we are considering a steady periodic flow. The wave-number is complex, $\bar{\alpha} = \bar{\alpha}_{re} + i\,\bar{\alpha}_{im}$ where $\bar{\alpha}_{re} = 2\pi/\lambda$ is the wave-number and $\bar{\alpha}_{im}$ is the spatial disturbance amplification rate. The functions $\phi(\eta, x)$ and $s(\eta, x)$ are the dimensionless velocity and temperature disturbance amplitude function for the disturbances. The similarity variable is $\eta = y/\delta$.

Appropriate non-dimensionalization for

length, velocity and temperature functions may be obtained by using the characteristic quantities of the base flow (see Pera and Gebhart [1]).

$$\delta \equiv \frac{5x}{G^+} \tag{7}$$

$$U^* \equiv \frac{\nu {G^+}^2}{5x} \tag{8}$$

$$\Delta t = t_0 - t_\infty . \tag{9}$$

The relevant Grashof number and its more convenient form G^+ are

$$Gr_x = \frac{g\beta x^3 \Delta t \cos\theta}{\nu^2}, G^+ = 5 \sqrt[5]{\left(\frac{Gr_x}{5}\right)}.$$

The disturbance quantities are generalized as $\alpha = \bar{\alpha}\,\delta$ and $\beta = \bar{\beta}\delta/U^*$.

The resulting vorticity equation, from (2) and (3), and the energy equation (4), when linearized with respect to the disturbance quantities reduce, to the following form in disturbance amplitude functions ϕ and s.

$$(f' - \beta/\alpha)(\phi'' - \alpha^2\phi) - f'''\phi = \frac{1}{i\alpha G^+}$$

$$\times (\phi'''' - 2\alpha^2\phi'' + \alpha^4\phi - s'\varepsilon) - \frac{s}{5} \tag{10}$$

$$s'' - \alpha^2 s = i\alpha Pr\, G^+ [(f' - \beta/\alpha)\, s - \phi\Phi'] \tag{11}$$

where the independent variable is $\eta = (y/5x)\, G^+$. The perturbation parameter ε is a function of the strength of the local flow and of the amount of surface inclination. Pera and Gebhart [1] found this parameter and indicated its region of physical validity. It is zero for a horizontal surface. For a surface inclined at an angle of θ with respect to the vertical it is

$$\varepsilon(x) = \tfrac{1}{5} G^+ \tan\theta.$$

In equations (10) and (11) the ratio β/α is the complex wave velocity and G^+ indicates the local vigor of the flow. The appropriate boundary conditions for the disturbance amplitudes ϕ and s in equations (10) and (11) require that all distrubances vanish in the far field. Velocity distrubances are zero at the surface and, if the surface has large thermal capacity, the temperature distrubance is also zero there. Thus, we have

$$\phi(\infty) = \phi'(\infty) = s(\infty) = \phi(0) = \phi'(0) = s(0) = 0 \tag{12}$$

The coupled system of equations (10) and (11), with boundary conditions (12), were numerically integrated for a Prandtl number of 0·7 and for $\varepsilon = 0$, 0·25, 0·5, 0·75 and 1·0. The integration was started with the asymptotic solutions of the disturbance amplitude functions at the edge of the boundary layer and was continued to the surface. All parameters and eigenvalues were then adjusted to meet the specified surface conditions. The three linearly independent integral solutions of (10) and of (11), each of which decay exponentially for large η, were individually computed and recombined only at the surface, by the method of Hieber and Gebhart [3], where boundary conditions are to be satisfied. Denoting these integrals by ϕ_1, s_1 (uncoupled inviscid); ϕ_2, s_2 (uncoupled viscous); ϕ_3, s_3 (coupled viscous); one has at large η

$$\phi_1 \sim e^{-a\eta}, \quad \phi_2 \sim e^{-b\eta}, \quad \phi_3 \sim e^{-d\eta} \tag{13}$$

where b and d are:

$$b = \sqrt{(\alpha^2 - i\beta G^+)} \quad \text{and} \quad d = \sqrt{(\alpha^2 - i\beta G^+ Pr)}. \tag{14}$$

Since the asymptotic behavior of the base flow temperature profile is

$$\Phi' = -A \exp[-Pr(n+3)\, f_0(\infty)\, \eta] \tag{15}$$

where A is an appropriate constant that considers higher orders of approximation for the primary flow and $f_0(\infty)$, the first order boundary layer stream function evaluated at the edge of the boundary region is equal to 0·6462 for $Pr = 0{\cdot}7$. It follows from (13) and (11) that as, $\eta \to \infty$, the associated temperature integrals are

$$s_1 \sim C_1 \exp\left[-\{(n+3)Prf_0(\infty) + \alpha\}\eta\right]$$
$$s_2 \sim C_2 \exp\left[-\{(n+3)Prf_0(\infty) + b\}\eta\right] \quad (16)$$
$$s_3 \sim C_3 \exp\left[-d\eta\right]$$

where C_1, C_2 and C_3 are computable constants.

Denoting the composite solution by

$$\phi = \phi_1 + A\phi_2 + B\phi_3 \quad (17)$$

one proceeds to determine ϕ_1, ϕ_2, ϕ_3, (and, concommitantly, s_1, s_2, s_3) by numerically integrating equations (10) and (11) from the edge of the boundary layer to $\eta = 0$. The asymptotic behavior in (13) and (16) are used to start the solutions. Having determined the three independent integrals at $\eta = 0$, A and B are evaluated by applying the two surface boundary conditions

$$\phi(0) = 0 = \phi_1(0) + A\phi_2(0) + B\phi_3(0)$$
$$\phi'(0) = 0 = \phi_1'(0) + A\phi_2'(0) + B\phi_3'(0). \quad (18)$$

The third boundary condition at the surface

$$s(0) = 0 = s_1(0) + As_2(0) + Bs_3(0) \quad (19)$$

will in general not be satisfied. Supposing values of G^+ and β to be fixed, one iterates in α (the eigenvalue), repeating the process until this condition is also satisfied. This method consists, in effect, in locating a point in a two-dimensional space.

NUMERICAL RESULTS

Curves of neutral stability ($\alpha_{im} = 0$) and amplification contours ($\alpha_{im} < 0$) were obtained for both horizontal and slightly inclined isothermal surfaces, for $Pr = 0{\cdot}7$. Figure 1 is the stability plane for the completely horizontal orientation, in terms of the wave-number α_{re} as a function of the local flow strength G^+. The calculations were carried out to $G^+ = 200$ and, given the high amplification rates seen on Fig. 1, this range should include the region of practical interest.

The β, G^+ plane is seen in Fig. 2. Constant amplitude ratio contours are shown, instead of the amplification rate contours. The ratio contours are more useful for estimating actual

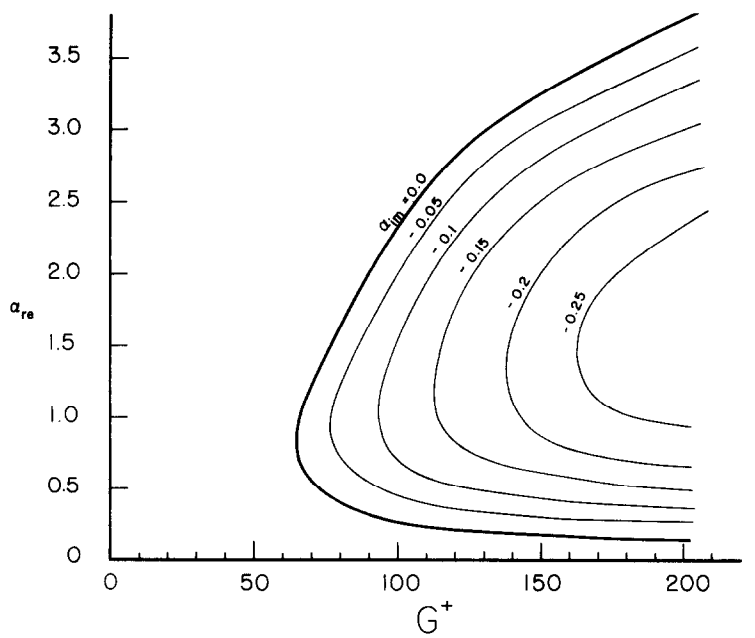

FIG. 1. Neutral stability curve and amplification rate contours for the natural convection flow adjacent to a uniform temperature horizontal surface. $Pr = 0{\cdot}7$.

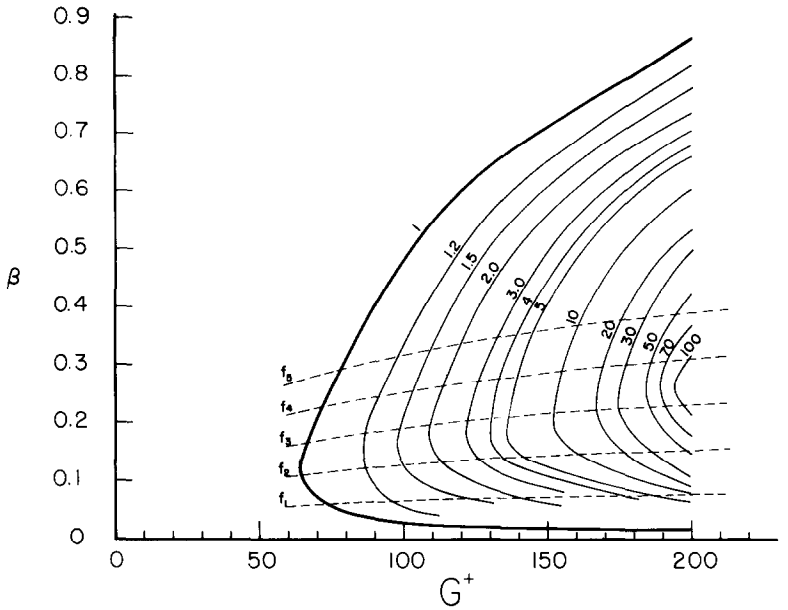

FIG. 2. Neutral stability curve and amplitude ratio contours for the natural convection flow adjacent to a uniform temperature horizontal surface. $Pr = 0{\cdot}7$. Also shown as dotted lines are several paths of constant disturbance frequency.

disturbance growth and in discerning any effect of frequency filtering. The amplitude ratio is calculated in the manner of Dring and Gebhart [17] as follows. Consider a disturbance of given physical frequency and having amplitude A_1 at the location where the strength of the local flow is G_1^+, the amplitude of the same distrubance at G^+ is calculated by the following relation:

$$\frac{A_2}{A_1} = \exp\left\{-\frac{1}{5}\int_{G_1^+}^{G^+} \alpha_{\text{im}}\, dG\right\}.$$

This integration proceeds along the path that a disturbance of any given physical frequency $\bar{\beta}$ follows from the neutral curve at $G_1^+(\beta)$, and into the unstable region, as it is convected downstream. The path of a disturbance of constant physical frequency on β, G^+ coordinates $\beta G^{+-\frac{1}{2}} = \text{constant}$, from the generalization of $\bar{\beta}$ given above. Several such paths are shown as dotted lines in Fig. 2. Contours of constant A_2/A_1 are seen. The number that characterizes a constant amplitude ratio contour is the amplitude that a disturbance will have as it crosses that contour, at G^+, if it had an amplitude of one when it crossed the neutral curve.

The highest value of A_2/A_1 shown is at about $G^+ = 200$. Note that the disturbance which is first unstable, approximately f_2, is not the one which is the most highly amplified. A narrow band of somewhat higher frequencies is much more important. This is the same filtering mechanism found by Dring and Gebhart [17] to be very selective for flow adjacent to vertical surfaces but not found to be strong by Pera and Gebhart [18] for plane plume flows.

The neutral stability curves for slightly inclined surfaces are given in Fig. 3 in terms of the frequency parameter β. Surface inclination is indicated by the expansion parameter ε, which is a function of the strength of the local flow (G^+) and of the surface inclination (θ). Neutral curves are given in the range of ε from 0 to 1·0. Constant frequency contours are again shown as dotted lines. As the perturbation parameter increases, it is seen that the neutral curves shift to the right.

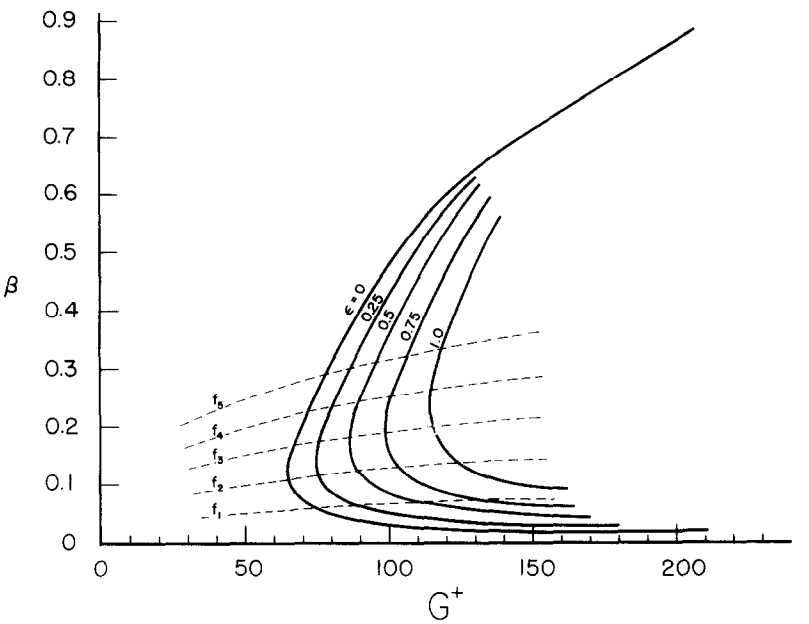

FIG. 3. Neutral stability curves for the natural convection flow adjacent to a uniform temperature horizontal and nearly horizontal surface. Surface inclinations are represented by ε. $Pr = 0{\cdot}7$. Several paths of constant disturbance frequency are shown.

Thus, inclination stabilizes the flow. Another important characteristic is apparent from Fig. 3. The sharpness of the nose of the neutral curve for a horizontal surface indicates sharp frequency filtering. As ε increases the nose of the neutral curve becomes flatter and the width of the band of favored frequencies presumably becomes wider.

These results may be generalized to determine the effect that combined agencies of buoyancy, such as thermal and chemical species diffusion, have on stability and on disturbance growth rates for such laminar flows. This question is considered next.

THE EFFECT OF A DIFFUSING CHEMICAL SPECIES ON STABILITY

There are numerous transport processes in nature in which natural convection flows are caused by a combined effect of temperature gradients and concentration gradients of a diffusing chemical species. On the surface of the earth, for example, the diffusion of the water vapor to the atmosphere may have a large effect on the natural convection flow which results from temperature inhomogeneities.

There are many kinds of other flow circumstances, especially in the natural environment, which result from a combination of buoyancy mechanisms. Some of the most important kinds of mass diffusion arising in air were considered by Pera and Gebhart [19], for horizontal surfaces. Laminar boundary layer flow was analyzed for a range of Schmidt number from 0·1 to 10, where $Sc = \nu/D$, D being the molecular diffusivity of the diffusing species. This range includes most of the important applications in gases.

An additional interest in the study of such flows is the determination of the effect that combined agencies of buoyancy have on stability limits and on disturbance growth rates. We will limit our consideration to flows for which $Pr = Sc$, since such stability limits may be simply derived from those calculated above.

Gebhart and Pera [16] have shown that a

simple similarity formulation accounts for the combined action of the thermal and species diffusion effects when each are linearized in the sense of the Boussinesq approximation. If, in addition, $Pr = Sc$, then coupling effects through buoyancy may be written as either the thermal or the species diffusion term in the primary flow and stability equations. The only difference in this formulation is the meaning given to the local Grashof number. It becomes a combined one, $Gr_{x,t} + Gr_{x,C}$, where $Gr_{x,t}$ is the previously defined thermal Grashof number and $Gr_{x,C}$ is the local chemical species diffusion Grashof number. The wavelength and the frequency parameters are similarly generalized in terms of $Gr_{x,t} + Gr_{x,C}$. The stability limits and disturbance growth characteristics may, therefore, be obtained by a simple reinterpretation of the results computed with a single buoyancy mechanism. Here G^+ is simply taken as the combina- of the two effects.

However, these conclusions concerning stability do not apply for $Pr \neq Sc$. In this circumstance the two buoyancy mechanisms may not be thus combined because the thermal and species diffusion regions do not have the same distributions or completely overlap. Stability characteristics then must be obtained through numerical integration of the complete set of coupled momentum, energy and mass diffusion stability equations. This set is of eighth order.

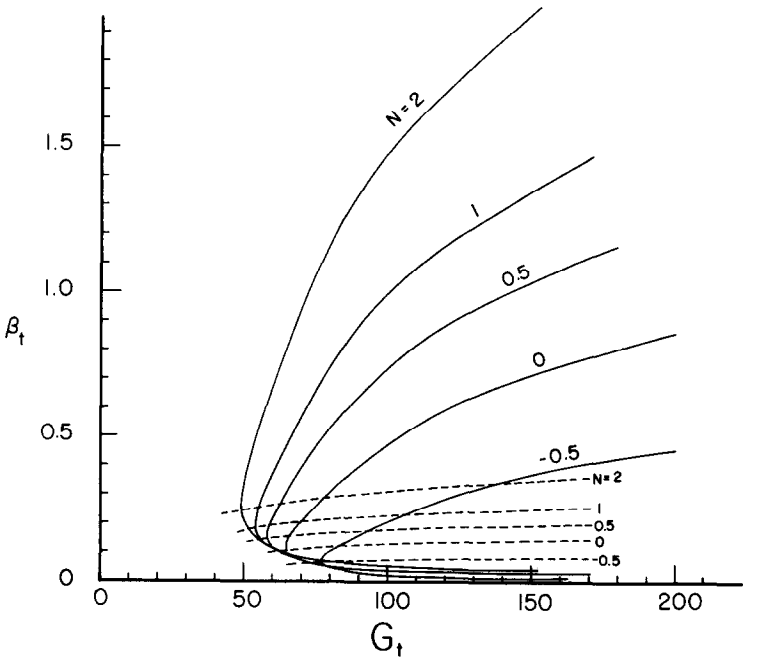

FIG. 4. Neutral stability curves for the natural convection flow adjacent to a horizontal surface with combined buoyancy effects. $Pr = 0{\cdot}7$. The temperature and concentration of the diffusing chemical species are constant, in x, at the surface.

Figure 4 shows a stability plane for $Pr = 0{\cdot}7$ and for flow adjacent to a horizontal surface.

These curves were derived from the neutral curve of Fig. 2. The neutral stability curves are shown for several values of the parameter $N = Gr_{x,C}/Gr_{x,t}$. Thus, N indicates the relative importance of the two parallel diffusion mechanisms. The coordinates are β_t and G_t^+, $\beta_t \propto \bar{\beta}x^2/\nu(Gr_{x,t})^{\frac{1}{2}}$ and $G_t^+ \propto (Gr_{x,t})^{\frac{1}{2}}$, i.e. $\bar{\beta}$ is generalized only in terms of the thermal buoyancy effect. The neutral curves of Fig. 4 indicate that an increase of an aiding species diffusion effect ($N > 0$), i.e. a buoyancy effect added to a given level of thermal effect (seen at $N = 0$), destabilizes the flow and increases the physical frequency of the most unstable disturbance. When the two driving mechanisms oppose each other ($N < 0$) the flow is further stabilized.

THE EXPERIMENT

The stability characteristics discussed above concern two-dimensional disturbances. This initial approach to the question of laminar stability is reasonable in the event that two-dimensional disturbances are unstable at lower Grashof numbers than are three-dimensional ones. An argument similar to Squire's theorem, which was originally established for forced-flow boundary layers, has been successfully extended by Knowles and Gebhart [20] to vertical natural convection flows adjacent to surfaces. The same conclusions appears to apply for plane plumes. This question is much more difficult for the flows considered here. However, past experimental studies indicate that, for natural convection flow adjacent to surfaces much inclined from the vertical, three-dimensional effects very rapidly become important and that they may not be ignored in considering all details of such flows. Therefore, an experiment was necessary to ascertain the validity and applicability of the above calculations concerning two-dimensional disturbances and to study any additional mechanisms which might arise in particular three dimensional effects.

A series of experiments was carried out with the plate assemblies shown in Fig. 5, each maintained at uniform temperature. Details of the test surfaces seen in Figs. 5a and b are described in detail by Pera and Gebhart [1] in a study of attached laminar boundary layer flow over such surfaces. The observations made in that study indicated a need for a detailed consideration of the stability of such flows and of the nature of eventual separation.

These observations led to the plate design shown in Fig. 5c. It consists of two aluminium plates of 14 in. width and 9·5 in. length, hinged at their common edge. Each one is heated by six electrical strip resistance heaters embedded in the bottom. The electrical power dissipated by each heater was individually adjusted to obtain a uniform surface temperature condition, as determined by thermocouples. The strip heaters were cemented in channels machined on the lower side of the plate as shown in Fig. 5a. Between each heater a deep groove was opened from the bottom of the plate to reduce the heat conduction in the longitudinal direction (x) and to result in more sensitive control of the nonuniform surface heat fluxes which would maintain a uniform-surface temperature condition. Insulation material was mounted along the sides of the plate, and flush with the surface, to prevent vertical flow up over the edges. The bottom of the plates were also well insulated. The two plates were V-edged at their contact. Thus the common edge could be raised, by a lifting mechanism, to provide a continuous range of surface inclinations from zero to about twenty degrees above the horizontal. The result was a symmetric wedge-shaped geometry with two leading edges. For both the one or two leading-edge surface configurations, Figs. 5b and c, high quality glass side walls were used as shown to prevent any edge flows. The flow from the leading and trailing edges was not impeded.

The surface temperature of the hinged plate was measured with twelve copperconstantan thermocouples, six on each of the two sections. Each was located above a heater strip heater and approximately at 0·010 in. below the exposed surface. These thermocouples were used to

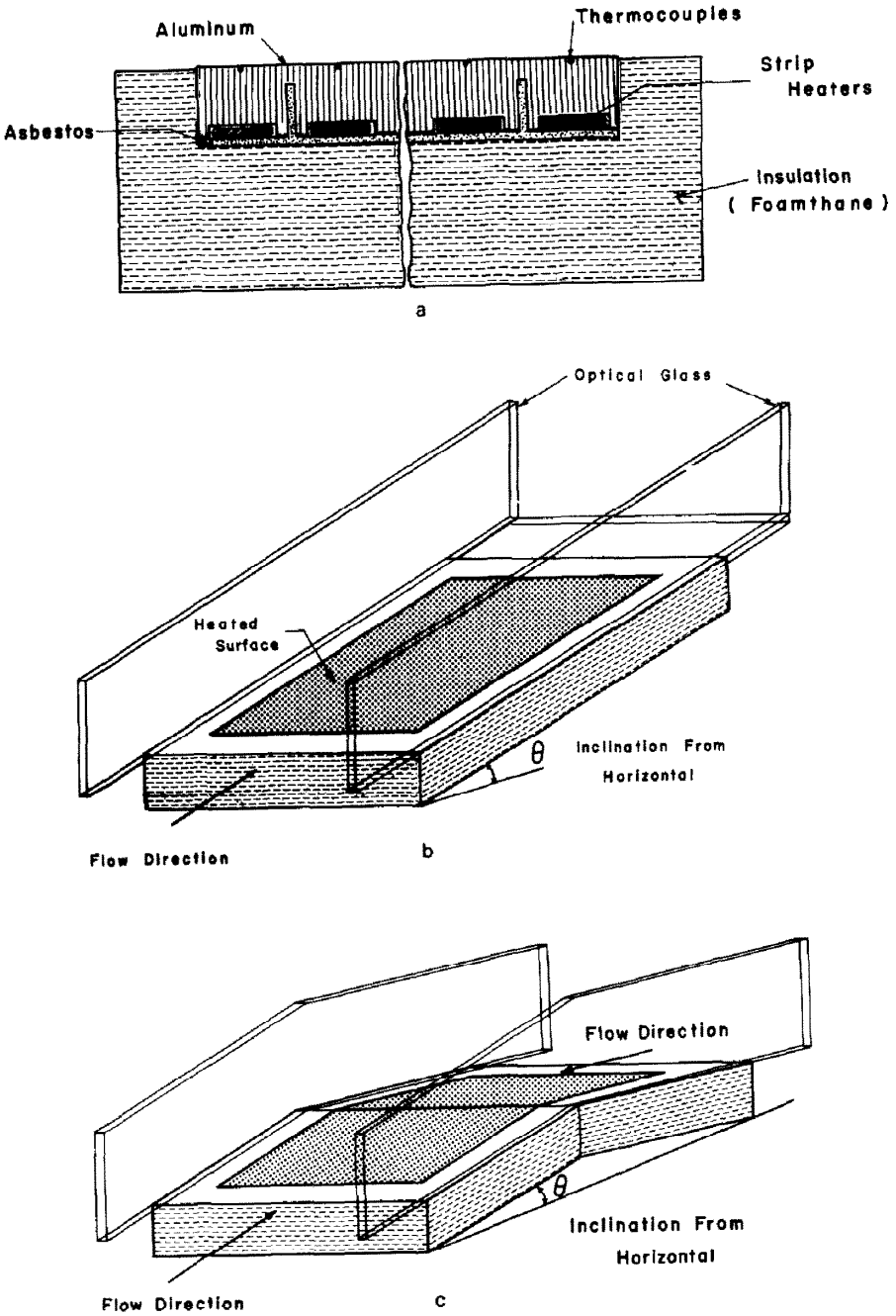

FIG. 5. Diagrams of the uniform temperature surfaces. (a) Section showing heaters, grooves and insulation. (b) General view, one leading edge configuration. (c) General view, two leading edges configuration.

check for surface temperature uniformity, which was maintained within 0·2°F during the runs.

Observations were made with a 5 in. Mach-Zehnder interferometer, fitted with a Mercury-vapor light source having a green interference filter. Adjustment was made to the infinite fringe, thus each fringe was approximately an isothermal contour. For a two-dimensional temperature field 14 in. wide, in air at atmospheric conditions, the interferometer sensitivity was about 3·6°F per fringe. The agreement between the surface temperatures determined by interferometric analysis and by thermocouple readings was always within 0·8°F. This validated the assumption that the width of the disturbed optical path was equal to the width of the plate (14 in.).

For air ($Pr = 0{\cdot}7$), the thickness of the temperature field normal to the surface is approximately equal to that of the velocity field. This is important in the interpretation of stability characteristics determined purely from interferometric determinations.

EXPERIMENTAL RESULTS AND DISCUSSION

The first experiments concerned the undisturbed natural convection flow over horizontal and slightly inclined surfaces. We wished to determine what conditions affect the nature and extent of the attached boundary layer region.

The influence that the downstream conditions may have on the upstream flow was first studied. An adiabatic trailing edge was used as shown in Fig. 5b. This removable adiabatic extension of the flat surface reached 12 in. beyond the heated surface. Temperature distributions were determined with the interferometer both with and without the adiabatic trailing edge. No noticeable differences were detected over a range of surface inclination from 0 to 20 degrees. This observation is in agreement with the experimental findings of Hassan and Mohamed [15], also for inclined surfaces.

The attached boundary region temperature distributions adjacent to the ridge-shaped surface of Fig. 5c were also compared with those adjacent to the surface of Fig. 5b, under equivalent flow conditions. Differences were within the experimental accuracy and repeatibility of the temperature distribution results (better than 1 per cent). Thus, various different trailing edge conditions were found to have no appreciable effect upstream, over a wide range of surface inclinations.

For the three experimental conditions studied, with and without a trailing edge, and with the symmetric surface geometry, the boundary layer was found to remain attached to the surface for only a short distance beyond the leading edge, for both a horizontal orientation and for small inclinations. The flow soon leaves the surface and rises. It eventually becomes a buoyant plume, after an initial phase of convective cells.

From our experimental results it may be concluded that different physical conditions imposed well beyond the occurrence of the flow. separation do not induce noticeable changes in the attached upstream region of such flow. We therefore conclude that the events leading to separation occur in the attached upstream flow. These observations appear to justify the comparison of experimental results obtained with various finite plate arrangements with the predictions of analyses which assume semi-infinite surfaces.

In both surface arrangements (Figs. 5b and c) the plates were provided with two-inch wide adiabatic extensions ahead of the leading edges. This was done to avoid the generation of an appreciable flow under the surface or against an opposed upstream face of the plate. Figure 6 is an interferogram of the leading edge region. It is seen that the boundary region does not start exactly at the beginning of the heated surface (dark vertical line), but begins some distance upstream. This results from heat conduction through the insulation material. This is an unavoidable effect in a fluid of such low thermal conductivity as air. A distance to a "virtual" leading edge was estimated to account for this effect.

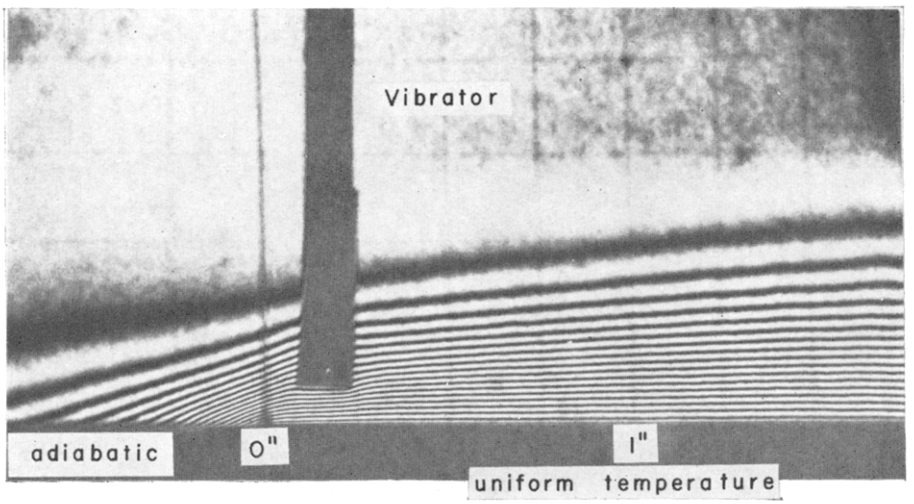

FIG. 6. Plate leading edge and vibrator. The darker vertical grid-line indicates the beginning of the heated surface. $\Delta t = 59{\cdot}6°F$. At the vibrator $G = 33$. Distance between each grid-line = 0·25 in.

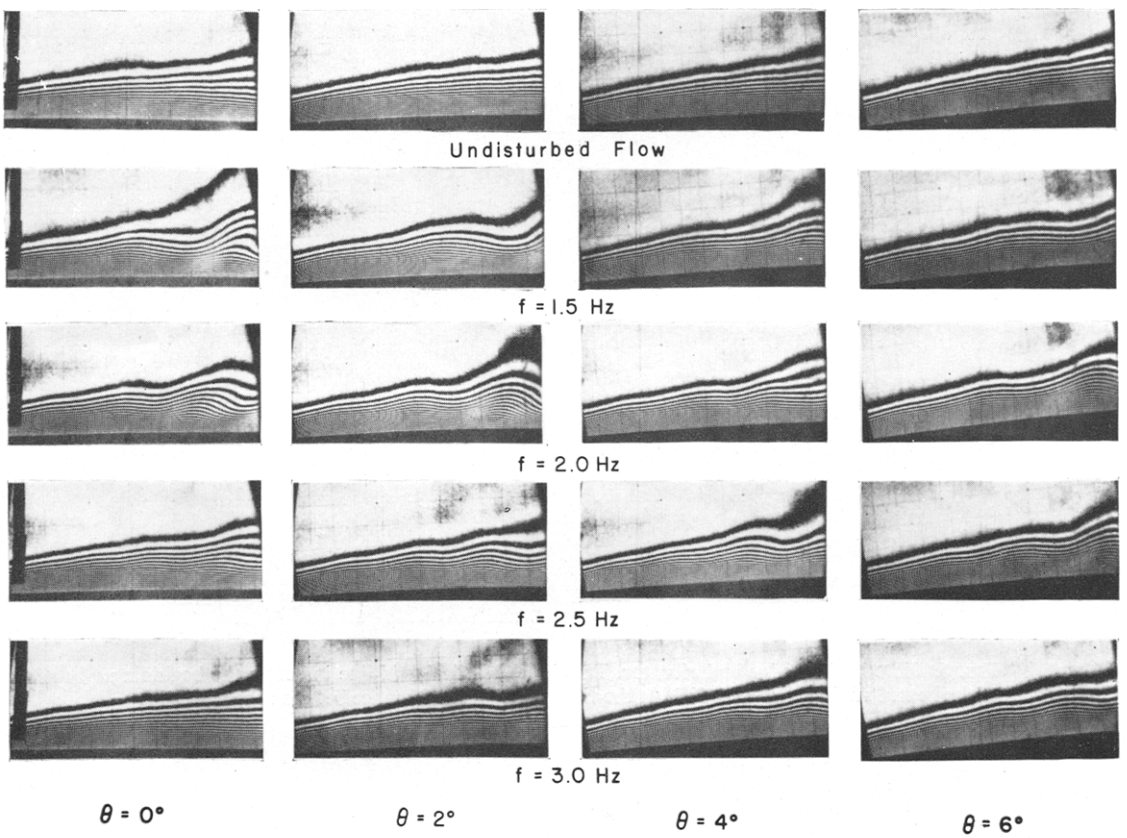

FIG. 7. Sequence of natural convection boundary-layer flows adjacent to a uniform temperature horizontal and inclined surface. Frequency of disturbances and angle of surface inclinations are indicated in the figure. $\Delta t = 56°F$.

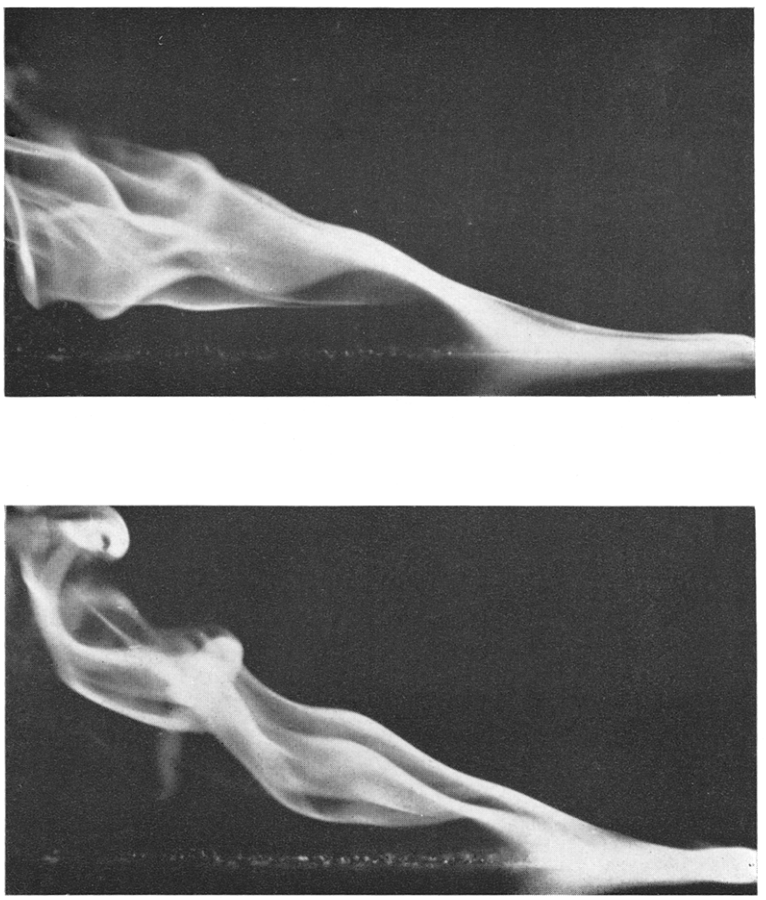

FIG. 8. Smoke streamline introduced into the flow over horizontal isothermal surface shows boundary-layer separation and three-dimensional effects. $\Delta t = 56°F$. Flow toward left.

(a) Undisturbed flow.

(b) Attached flow oscillated with a small sinusoidal disturbance of 1·7 Hz.

The second part of the experiments was a study of the stability and separation of the attached boundary layer flow formed over the first part of the plate. Stability characteristics were assessed by introducing small, controlled and approximately sinusoidal disturbances into the boundary layer. A vibrating ribbon was used and the frequency and amplitude of its oscillation were controlled. The ribbon support is seen in Fig. 6. A strip of metallic foil 0·005 in. thick and $\frac{1}{8}$ in. wide spans the plate between these supports and is normal to the plane of the photograph. Figure 6 indicates that the presence of the ribbon causes very little distortion when it is stationary. This method of introducing controlled disturbances into boundary layers has been previously used both in forced and natural convection flows with good results.

Figure 7 is a composite of interferograms of the boundary layer flow adjacent to the isothermal surface having a single leading edge. Inclinations of $\theta = 0, 2, 4$ and $6°$ are shown with ribbon frequencies of 1·5, 2·0, 2·5 and 3·0 Hz. These interferograms are representative of the many interferometric measurements taken. This collection together illustrates several of the most important observations made concerning flow and stability.

First, it is seen that, as the surface inclination increases, the boundary layer becomes thinner and more regular. This is best seen in the undisturbed flows across the top of the figure. During these studies we often saw natural disturbances in the boundary layer. They appeared very irregularly. They usually amplified and sometimes even momentarily disrupted the flow. However, such disturbances are not present in the collection of Fig. 7.

The response of the boundary layer to small controlled two-dimensional disturbances, as a function of inclination and frequency is apparent in the sequences of Fig. 7. Our initial studies had indicated that disturbances in the frequency band 1·5–3·0 Hz were the most highly amplified, for our experimental conditions. With the surface horizontal ($\theta = 0°$), it is seen that the disturbance which amplified most rapidly, among those shown, is the one with a frequency of 1·5 Hz. The amplification rate sharply decreases as the disturbance frequency is increased. It also was found to decrease with decreasing frequency, not shown. At 3 Hz, for example, no appreciable amplification is seen.

As the surface inclination increases, the most rapidly amplified frequency also increases. For $\theta = 2°$ the critical frequency is about 2 Hz and becomes about 2·5 Hz for an inclination of 4°. Figure 7 also indicates that the bandwidth of highly amplified frequencues increases with inclination. Compare the results of $\theta = 0°$ and $\theta = 6°$. For $\theta = 6°$, amplification is seen for all the frequencies in the range 1·5–3·0 Hz. Amplification was also observed for frequencies higher than 3 Hz. However, for $\theta = 0°$ the band is much narrower.

These characteristics of frequency response are in reasonably good agreement with our theoretical results. The stability plane, Fig. 3, predicts that the most unstable frequency does increase with surface inclination $\varepsilon(x) \propto \tan\theta$. The band of most unstable frequencies also broadens with increasing inclination as indicated by the vertical broadening of the nose of the neutral curve as ε increases.

Similar experimental results were obtained when the adiabatic trailing edge was attached to this plate and also when the ridge geometry of Fig. 5c was used. These observations confirmed our earlier conclusion that conditions downstream of the flow separation region do not have a large effect on the stability in the attached upstream boundary layer flow.

The trends of the experimental results are consistent with the theory. However, the frequencies of the disturbances which actually undergo highest amplification are in some disagreement with stability calculations. For example, the frequencies f_1, f_2 and f_3 in Fig. 2 ($\theta = 0°$) correspond to about 1·5, 3 and 4·6 Hz, for our experimental conditions. Thus, the disturbance which we observed to undergo maximum amplification, actually about 1·7 Hz,

traverses the region slightly below the nose of the neutral curve and below the path of maximum amplification, which occurs at 2·8 Hz. Also, the location along the surface where disturbance growth is first observed was, for all flows, slightly to the left side of the neutral curve, i.e. in the region still predicted to be stable by the theory. Similar differences were also found adjacent to inclined surfaces.

These disagreements between calculations and experiment are greater than those found for vertical natural convection flows, as summarized by Gebhart [2]. This suggests that other, perhaps three-dimensional, effects may be very important here. If this is true, as has been suggested for flows adjacent to inclined surfaces much nearer vertical (Sparrow and Husar [11]) then there must be two co-existent modes of instability. A two-dimensional one must couple with a spanwise effect to perhaps produce a longitudinal cellular motion. The exchange of energy between various disturbance modes, and eventual flow separation, may be the cause of the discrepancies we have found between the two-dimensional linear theory and the actual experimental results.

We subsequently carried out a further study of three-dimensional and secondary flow effects. A different approach was necessary since interferograms average in the spanwise direction and are not a sensitive indicator of the consequences of any three-dimensional features which may arise in the flow. Smoke filaments were introduced into the attached flow near the leading edge of the surface. The typical smoke patterns are seen in Fig. 8, for the horizontal orientation. The lower picture shows such a flow, subject to a controlled disturbance in the attached flow region. It is seen that ordered three-dimensional effects are more clearly apparent than in the flow above. The smoke patterns are seen to roll and oscillate, even in the separated region. The frequency there is exactly that introduced by the vibrator. The rolling effect is apparent well upstream in the attached portion of the flow.

As seen, this boundary region flow undergoes some kind of separation, both without and with introduced disturbances. Pera and Gebhart [21] consider the nature and meaning of flow separation in natural convection flows. Detailed observations were made of flows leaving a heated cylindrical surface submerged in a quiescent body of water. They indicated that the mechanism of separation is very different than that usually occurring in forced flow. In buoyancy induced flows the flow turns away from the surface under increasing action of a component of the buoyancy force normal to it. No flow reversal is apparent. The pressure field which changes flow direction is generated internal to the flow layers and immediately adjacent to the surface, not in the external region, as in forced flows.

Figures 9 and 10 summarize our observations concerning boundary-layer separation and the beginning of cellular convection, in terms of the parameters Gr_x and Ra_δ. The Rayleigh number is based on the calculated local boundary layer thickness δ. Approximate locations for the onset of flow separation and for complete separation

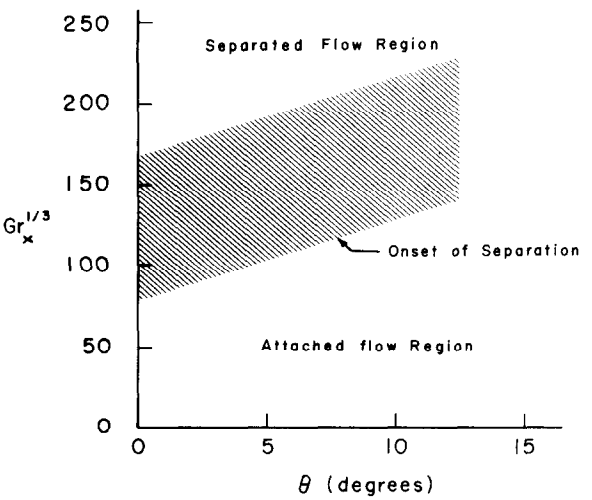

FIG. 9. Experimental determination of boundary layer separation in terms of the Grashof number, over horizontal and slightly inclined surfaces in air. The shadowed band indicates the region of intermittency between attached and cellular convective mechanisms. $\Delta t = 60°F$.

were determined at several surface inclinations, using a smoke indicator. It was clear that boundary-layer separation at a given inclination did not always occur at the same location. The process is very unsteady. The location of separation moves downstream, convected by the flow, to leave behind a region of attached undisturbed flow. Eventually separation returns upstream and then is again convected away. Figures 9 and 10 show the range of local Grashof

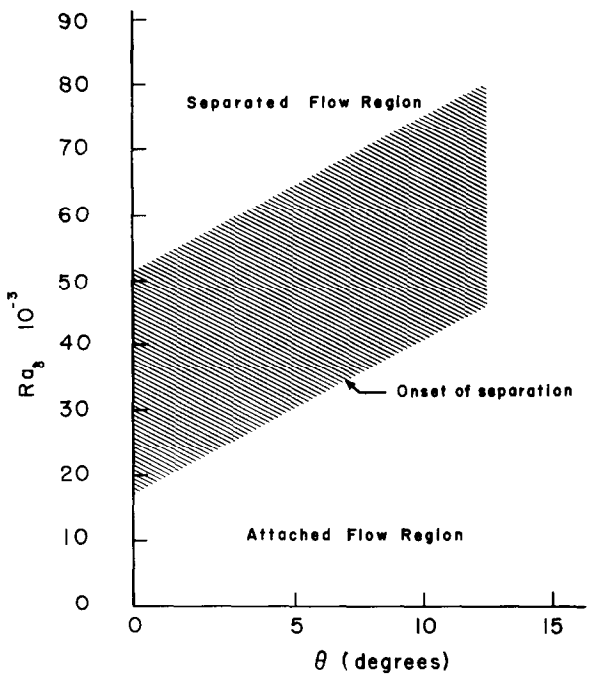

FIG. 10. Experimental determination of boundary layer separation in terms of the Rayleigh number over horizontal and slightly inclined surfaces in air. The shadowed band indicates the region of intermittency between the attached and cellular convective mechanisms. $\Delta t = 60°F$.

and of Rayleigh numbers (locations) in which, for our experimental conditions, flow separation was found. Locations above the band shown were always completely separated flow. This region was dominated by unsteady cellular convection. The flow was always attached below the band. These same results were found for both surface arrangements, i.e. for the single surface and for the symmetric, or ridged, one.

For a horizontal surface ($\theta = 0$) the earliest onset of boundary layer separation was at $Gr_x^{\frac{1}{4}}$ of about 80. This value corresponds to a G^+ of 50. A flow of this strength was calculated by stability theory to be still stable to small two-dimensional disturbances, see Fig. 2. We see in Fig. 9 that, as the surface inclination increases, the region of the first occurrence of boundary layer separation and of complete flow separation move downstream. For an inclination of 12 degrees, the first separation occurs at about a $Gr_x^{\frac{1}{4}}$ of 130. Our value of $Gr_x^{\frac{1}{4}} = 80$ at the first occurrence of separation for $\theta = 0$ is in good agreement with that found by Rotem and Claassen [14] with a Schlieren system.

Separated region flow was found to be very different in the two surface assemblies investigated. Over the single surface the flow separates as shown in Fig. 8 and then rises. After separation the flow is dominated by an unsteady cellular motion, without regular convection patterns or a preferred location for rising. For the double inclined, or ridged, surface, flow separation occurs in a similar way, but the separated flows instead meet and rise as a single plume near the plane of symmetry of the plate assembly. Such differences would appear to be important in flows which commonly occur in the natural environment, especially those formed above ridged earth surfaces. These flows are very important in atmospheric mixing and in the general dispersion of local temperature and concentration gradients.

ACKNOWLEDGEMENTS

The authors wish to acknowledge support from the National Science foundation under Research Grant GK-18529 for this research. The first author wishes to acknowledge support as a Graduate Research Assistant from the same grant.

REFERENCES

1. L. PERA and B. GEBHART, Natural convection boundary layer flow over horizontal and slightly inclined surfaces, *Int. J. Heat Mass Transfer* **16**, 1131–1146 (1973).
2. B. GEBHART, *J. Heat Transfer* **91**, 293 (1969).
3. C. A. HEIBER and B. GEBHART, *J. Fluid Mech.* **48**, 625–646 (1971).
4. B. R. RICH, *Trans. ASME* **75**, 489 (1953).

5. J. F. CROFT, *Q. R. Met. Soc.* **84**, 418 (1958).
6. D. J. TRITTON, *J. Fluid Mech.* **16**, 417 (1963).
7. D. J. TRITTON, *J. Fluid Mech.* **16**, 282 (1963).
8. G. S. H. LOCK, C. GORT and G. R. POND, *Appl. Sci. Res.* **18**, 171 (1967).
9. R. B. HUSAR and E. M. SPARROW, *Int. J. Heat Mass Transfer* **11**, 1206 (1968).
10. D. J. BAKER, *J. Fluid Mech.* **26**, 573–575.
11. E. M. SPARROW and R. B. HUSAR, *J. Fluid Mech.* **37**, 251 (1969).
12. J. R. LLOYD and E. M. SPARROW, *J. Fluid Mech.* **42**, 465 (1970).
13. J. E. PLAPP, Laminar boundary layer stability in free convection, Ph.D. Thesis, Calif. Inst. Tech. (1957).
14. F. ROTEM and L. CLAASSEN, *J. Fluid Mech.* **39**, 173. See also *Can. J. Chem. Engng* **47**, 461–468 (1969).
15. K. E. HASSAN and S. A. MOHAMED, *Int. J. Heat Mass Transfer* **13**, 1873 (1970).
16. B. GEBHART and L. PERA, *Int. J. Heat Mass Transfer* **14**, 2025–2050 (1971).
17. R. DRING and B. GEBHART, *J. Fluid Mech.* **34**, 551–564 (1968).
18. L. PERA and B. GEBHART, *Int. J. Heat Mass Transfer* **14**, 975–984 (1971).
19. L. PERA and B. GEBHART, *Int. J. Heat Mass Transfer* **15**, 269–278 (1972).
20. C. P. KNOWLES and B. GEBHART, *J. Fluid Mech.* **34**, 657 (1968).
21. L. PERA and B. GEBHART, *Int. J. Heat Mass Transfer* **15**, 175–177 (1972).

SUR LA STABILITE DE L'ECOULEMENT PAR CONVECTION NATURELLE AVEC COUCHE LIMITE AU-DESSUS DE SURFACES HORIZONTALES ET LEGEREMENT INCLINEES

Résumé—Voici une étude théorique et expérimentale de l'écoulement par convection naturelle avec couche limite adjacente à des surfaces soit horizontales soit légèrement inclinées. Les effets d'Archimède additionnels résultant des petites inclinaisons de surface ont été considérés ainsi que l'effet d'Archimède additionnel apparaissant dans la diffusion d'espèces chimiques. On a déterminé les limites et les conditions pour l'écoulement avec couche limite attachée. On a étudie le cas de la séparation de l'écoulement.

La stabilité de cet écoulement vis-à-vis de perturbations bi-dimensionnelles est étudiée a l'aide de la théorie linéaire de stabilité. Les contours de stabilité neutre et du taux d'amplification sont obtenus par intégration numérique des équations de stabilité couplées de quantité de mouvement et d'énergie pour l'air ($Pr = 0{,}7$). L'effet sur la stabilité d'une petite inclinaison de la surface est étudié en utilisant les résultats de l'analyse de perturbation pour de tels écoulements. On a trouvé aussi l'effet de la diffusion simultanée de masse dans le cas de nombres de Prandtl et de Schmidt égaux.

Une vérification expérimentale des calculs de stabilité a été faite en perturbant les écoulements dans un domaine de fréquence avec un mince ruban vibrant et en observant le comportement de la perturbation convectée. On a utilisé un interféromètre Mach–Zehnder pour étudier les caractéristiques de l'écoulement à la fois dans les conditions perturbées ou non. Les perturbations tridimensionnelles les plus complexes ont été rendues visibles par injection de fumée dans la région frontière.

La théorie de la stabilité prédit correctement les limites de stabilité à la fois pour des surfaces horizontales et légèrement inclinées. Néanmoins, les calculs ne sont pas en aussi bon accord avec les observations que dans le cas d'écoulements adjacents à des surfaces verticales ou de panaches s'élevant par convection naturelle. On pense que les désaccords trouvés résultent de la croissance rapide des effets tridimensionnels dans la région de couche limite attachée et d'un phénomène de retour semblable à une séparation.

ÜBER DIE STABILITÄT DER GRENZSCHICHT BEI FREIER KONVEKTION AN EINER LEICHT GENEIGTEN, HORIZONTAL ÜBERSTRÖMTEN OBERFLÄCHE

Zusammenfassung—Dies ist eine analytische und experimentelle Untersuchung über die Stabilität der Grenzschicht bei freier Konvektion an einer leicht geneigten, horizontal überströmten Oberfläche. Die zusätzlichen Auftriebseffekte, bedingt durch die kleine Schrägstellung der Oberfläche, wurden berücksichtigt. Ferner wurde die Wirkung eines zusätzlichen Auftriebs infolge der Diffusion aufgrund chemischer Wirkung betrachtet. Die Grenzen und Bedingungen für haftende Strömungsgrenzschichten sind angegeben. Die Frage nach der Strömungsablösung wurde untersucht.

Die Stabilität dieser Strömung bei zweidimensionalen Störungen wurde mit der linearen Stabilitätstheorie untersucht. Neutrale Stabilitätsgrenzen und der Verlauf des Verstärkungsfaktors wurden erhalten durch numerische Integration der durch Kopplung von Bewegungs- und Energiegleichung entstehenden Stabilitätsgleichung achter Ordnung für Luft ($Pr = 0{,}7$). Der Einfluss einer kleinen Neigung der Oberfläche auf die Stabilität wurde untersucht unter Verwendung der Ergebnisse einer Störungsanalyse dieser Strömung.

Der Einfluss einer gleichzeitigen Stoffübertragung auf die Stabilität wurde auch festgestellt für den Fall gleicher Prandtl- und Schmidt-Zahl.

Der experimentelle Nachweis des berechneten Stabilitätsverhaltens wurde geführt durch Störung einer Strömung mit einem dünnen über einen Frequenzbereich schwingenden Streifen und durch Beobachtung des Verhaltens der eingeleiteten Störungen. Mit einem Mach-Zehnder-Interferometer wurden die Strömungscharakteristiken sowohl bei gestörten wie bei ungestörten Bedingungen untersucht.

Die ebenfalls auftretenden komplizierteren dreidimensionalen Störungen wurden durch Einblasen von

Die Stabilitätstheorie liefert die richtige Tendenz für die Stabilitätsgrenzen, sowohl für die horizontale wie auch für die leicht geneigte Oberfläche. Trotzdem stimmen die Berechnungen mit den Beobachtungen nicht so gut überein wie bei Strömungen entlang einer senkrechten Oberfläche oder in frei aufsteigenden thermischen Schlieren. Es wird vermutet, dass die gefundenen Diskrepanzen auf das schnelle Anwachsen dreidimensionaler Effekte im anliegenden Grenzschichtbereich und durch stromabwärts auftretende Aufspaltungsphänomene zurückzuführen sind.

ОБ УСТОЙЧИВОСТИ ТЕЧЕНИЯ В ПОГРАНИЧНОМ СЛОЕ НА ГОРИЗОНТАЛЬНЫХ И СЛЕГКА НАКЛОННЫХ ПОВЕРХНОСТЯХ ПРИ ЕСТЕСТВЕННОЙ КОНВЕКЦИИ

Аннотация—Проведено аналитическое и экспериментальное исследование устойчивости течения в пограничном слое на горизонтальных и слегка наклонных поверхностях при естественной конвекции. Учтены дополнительные эффекты подъёмной силы, возникающие при небольших наклонах поверхности. Кроме того рассматривается влияние дополнительной подъёмной силы, возникающей в результате диффузии химических веществ. Определены пределы и условия течения присоединенного пограничного слоя. Рассматривается проблема отрыва течения.

На основе линейной теории устойчивости изучалась устойчивость такого течения при двумерных возмущения. Кривые нейтральной устойчивости и коэффициент усиления найдены путём численного интегрирования полученной системы восьмимоментных конечных уранений устойчивости для количества движения и энергии для воздуха ($Pr = 0{,}7$). Влияние небольшого наклона поверхности на устойчивость изучалось на основании результатов анализа возмущения таких потоков. Кроме того было определено влияние одновременной диффузии массы на устойчивость для случая, когда число Прандтля равно числу Шмидта.

Экспериментальная проверка расчётов устойчивости осуществлялась путём возмущения реальных течений в диапазоне изменения частоты в случае тонкой вибрирующей ленты и наблюдения за поведением переносимого возмущения. Для изучения характеристик возмущенного и невозмущенного потоков использовался интерферометр Маха-Цендера. Более сложные трехмерные возмущения были видны при вдуве струйки дыма в пограничную область.

Теория устойчивости правильно предсказывает пределы устойчивости как для горизонтальных, так и для слегка наклонных поверхностей. Однако, расчёты не настолько хорошо согласуются с наблюдениями, как в случае течений вблизи вертикальных поверхностей или свободно поднимающихся тепловых струй. Найдено, что расхождения возникают за счёт быстрого роста трехмерных эффектов в присоединенной области пограничного слоя и за счёт явления типа отрыва вниз по потоку.